Hindawi Publishing Corporation
Mathematical Problems in Engineering
Volume 2015, Article ID 372321, 10 pages
http://dx.doi.org/10.1155/2015/372321

Research Article

Numerical Simulation of Rod-Plate Gap Streamer Discharge in SF_6/N_2 Gas Mixtures Based on ETG-FCT Method

Min Li,[1] Feng Wang,[1] Fang Fang Zhao,[2] Song Zhi Xu,[1] Jing Min Fan,[1] Xiao Lin Chen,[1] and Chi Zhi Huang[1]

[1] *School of Electrical and Information Engineering, Hunan University, Changsha 410082, China*
[2] *College of Finance and Statistics, Hunan University, Changsha 410006, China*

Correspondence should be addressed to Min Li; limin_zhenqi@hotmail.com and Feng Wang; wangfeng55@263.net

Received 15 May 2015; Accepted 8 July 2015

Academic Editor: David Bigaud

The Euler-Taylor-Galerkin flux-corrected transport (ETG-FCT) algorithm for the numerical solution of particle transport equations is described, based on the method developed by Lohner to solve conservation equations in fluid mechanics, and its application is extended to gas discharge problems. To improve the efficiency of computing and reduce numerical error, the nonuniform triangular mesh method is introduced, and the continuity equation is solved by ETG-FCT. The new contributions in this paper include the development of the ETG scheme and its application to rod-plate gap streamer discharge in 50~50% SF_6/N_2 gas mixtures problems. Results are obtained: the spatial distributions of electron densities, positive ion densities, negative ion densities, photoelectron densities, and the electric field, respectively. The velocities of streamer propagations and the radius of streamer obtained from the proposed model are in good agreement with experimental and simulation results in literature. The results also prove that the ETG-FCT method is valid.

1. Introduction

SF_6 is widely used as gas insulation medium because of having excellent dielectric and arc-quenching properties. It is widely used in electrical equipment, such as gas-insulated switchgear, circuit breaker, and transformer [1, 2]. However, as one of six limited gases, SF_6 is a strong greenhouse gas, and its high degrees of chemical inertness and thermal stability are due in part to its energetically favorable molecular structure. For the development of environmentally being electric power equipment and system, novel gases or mixture gases are strongly required as the substitute of SF_6 gas. Therefore, the study of substitute of SF_6 gas or its low mixed gas discharge mechanism has been a hot topic in the field of high voltage [3–6]. Obviously, it is important to choose the efficient numerical methods to research the low SF_6/N_2 mixed gas discharge property, which is a benefit to further understanding the discharge mechanism; improving and enhancing the level of gas-insulated switchgear has a good prospect.

FCT method was first proposed in 1973 by Boris and Book [7], which was applied in the very steep shock-like gradients that appear in fluid calculations. In numerical studies, difficulties arise with the solution of the continuity equations, due to the fact that the particle spatial distribution changes dramatically in streamer head [8], and, as a result, a very accurate numerical technique is required to capture their development. Therefore, there are many researchers who have studied the streamer discharge process focusing on the suitable numerical algorithm of high resolution [9–11]. Dynamics of discharge gap region of the high pressure air, nitrogen, and SF_6 in an inhomogeneous electric field was investigated by Bychkov and Yastremskii [12]. Christophorou and Van Brunt have researched the effects of ion and electron transport parameters in SF_6/N_2 mixed gas streamer discharge [1]. Beloplotov et al. [13] have studied the kinetic process in the electric discharge in SF_6 by comparing the calculated and experimental results. Morrow used the finite difference flux-corrected transport method (FDM-FCT) to study the corona discharge process of SF_6 gas [14], and the results have shown that the initial electric field plays an important role in the development of plasma discharge. However, the FDM can only be applied on the uniform grid region with a low accuracy of calculation. Due to the fact that the finite difference method for the solution of the particle convection equation has serious numerical diffusion and spurious oscillation, Pfeiffer et al. [15] have introduced the FCT method into their study of SF_6/N_2 mixed gas plasma discharge process, which suppressed the problem effectively. Hallac et al., who first introduced the flux-corrected transport into finite element method, used adaptive diffusion coefficient to low-order scheme and applied it to the two-dimensional dynamic simulation plasma discharge [16].

Due to the fact that the particle transport equations are convection-dominated diffusion problems, the FDM and first-order scheme will bring large numerical oscillation. To prevent this, on the basis of previous studies, the ETG-FCT method which can prevent calculation error effectively is described in this paper. The method is applied to solve the particle transport equation. In this study a rod to plate electrode configuration is applied and 50-50% SF_6/N_2 mixed gas is used as an insulating medium.

2. Mathematical Method

2.1. Description of the Model. The gas molecule, electron, positive ion, and negative ion continuity equations including ionization, recombination, attachment, drift, diffusion, and photoionization are solved simultaneously with coupled Poisson's equation in two dimensions [17, 18]

$$\begin{aligned}
\frac{\partial N_e}{\partial t} + \nabla\cdot(v_e N_e) &= \nabla^2 (D N_e) + (\alpha-\eta) N_e |v_e| \\
&\quad - \beta N_e N_+ + S, \\
\frac{\partial N_-}{\partial t} + \nabla\cdot(v_- N_-) &= \eta N_e |v_e| - \beta N_- N_+, \\
\frac{\partial N_+}{\partial t} + \nabla\cdot(v_+ N_+) &= \alpha N_e |v_e| - \beta N_e N_+ - \beta N_- N_+ + S, \\
\nabla^2 \varphi &= -\frac{e}{\varepsilon}(N_+ - N_- - N_e), \\
E &= -\nabla\varphi,
\end{aligned} \tag{1}$$

where t is the time, v_e, v_-, and v_+ are drift velocity, and N_e, N_-, and N_+ are densities for the electron, positive ion, and negative ion, respectively. The symbols α, η, and β are electron ionization-collision coefficient, attachment coefficient, and recombination coefficient, respectively. They are usually significantly dependent on both the electric field-to-gas density (E/N) and the concentration of mixed gas content [1]. N is the neutral gas number density, D is electron diffusion coefficient, E is the electric field, φ is the electric potential, ε is the relative permittivity, and e is the electronic charge, respectively. S is the charged particle source term due to the photoionization, which is calculated by the model of

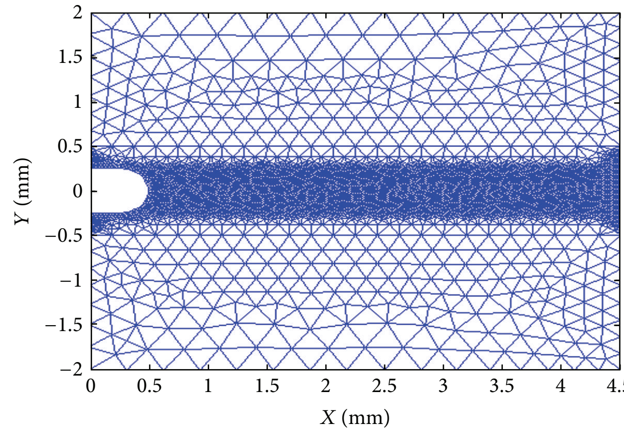

Figure 1: Finite element discretization (10254 elements).

[19]. The photoionization rate at point of observation (r, z) due to all source rings (r_s, z_s) in $\mathrm{cm}^{-3}\,\mathrm{s}^{-1}$ is

$$\begin{aligned}
S(r,z) &= \int dr_s \int dz_s \frac{p_q}{p_q + p} \alpha' v_e n_e \frac{r_s}{4\pi} \int_0^{2\pi} \frac{f(|r_\omega|)}{4\pi r_\omega^2} d\omega, \\
|r_\omega| &= \sqrt{(z - z_s)^2 + r_s^2 + r^2 - 2 r r_s \cos(\omega)},
\end{aligned} \tag{2}$$

where p_q is the partial pressure of mixed gas, p is the pressure of atmosphere, n_e is the electron number density, v_e is the velocity of the electron, α' is the excitation coefficient, which is proportional to the ionization α, and $f(|r_\omega|)/4\pi r_\omega^2$ is the emission probability of photons.

During the process of plasma formation and growth, the particle densities change markedly. Net charge has a great effect on the electric field. Moreover, the field varies strongly in both space and time, and the field is solved by using coupled Poisson's equation at each time step. To save computing time and memory, a nonuniform spatial triangular mesh is therefore essential for an accurate and efficient numerical treatment of discharge phenomena. There is a very fine spatial mesh in the streamer channel, and a very coarse grid is used on boundary and other regions. Figure 1 shows the finite element discretization (10254 elements).

2.2. ETG Scheme. The particle transport equations are a convection-dominated question. Using first-order linear scheme for solving convection-diffusion systems is more prone to causing large numerical diffusion or spurious oscillation. Therefore, in this paper, we expand $N(x, y, t)$ in a Taylor series to the third order in time, ignoring the more fourth-order items. And the discrete particle transport equations are solved by the FCT method. We only consider the effect of the convection term and assume that $\nabla\cdot v = 0$, and the advection equation expression is as follows:

$$N_t + \nabla\cdot(vN) = 0. \tag{3}$$

To develop a generalized Euler time-stepping scheme for (3), we employ a forward-time Taylor series expansion and its expression is as follows:

$$N(x,y,t_{n+1}) = N(x,y,t_n) + \Delta t N_t + \frac{\Delta t^2}{2} N_{tt} + \frac{\Delta t^3}{6} N_{ttt} + o(\Delta t^4). \tag{4}$$

By differentiation of (3) we have

$$N_{tt} = -\nabla\cdot(vN_t), \tag{5}$$

$$N_{ttt} = -\nabla\cdot(vN_{tt}). \tag{6}$$

So upon substitution of N_t with (3), N_{tt} with (5), and N_{ttt} with (6), semidiscrete equation (4) may be rewritten in the following form:

$$\begin{aligned} N^{n+1} - N^n &= -\Delta t\nabla\cdot(vN^n) - \frac{\Delta t^2}{2}\nabla\cdot(vN_t) - \frac{\Delta t^3}{6}\nabla \cdot(vN_{tt}) \\ &= -\nabla \cdot\left[v\left(\Delta t N^n + \frac{\Delta t^2}{2}N_t + \frac{\Delta t^3}{6}N_{tt}\right)\right], \end{aligned} \tag{7}$$

$$N^{n+1} - N^n = -\left[\Delta t v - \frac{\Delta t^2}{2}(v\cdot\nabla)v\right]\nabla N^n + \frac{\Delta t^3}{6}v \cdot\nabla(v\cdot\nabla N_t). \tag{8}$$

Equation (8) has an interesting structure. The first term on the right-hand side is a generalized convective term which accounts for the spatial variations of the velocity field. The last term in (8) originates from the third-time derivative term in Taylor series expansion and after substitution of N_t with $(N^{n+1} - N^n)/\Delta t$, it may be transferred to the left-hand side of the equation to produce the following generalized Euler time-stepping scheme:

$$\begin{aligned} \left\{1 - \frac{\Delta t^2}{6}v\cdot\nabla(v\cdot\nabla)\right\}\left(\frac{N^{n+1} - N^n}{\Delta t}\right) \\ = -\left[v - \frac{\Delta t}{2}(v\cdot\nabla)v\right]\cdot\nabla N^n. \end{aligned} \tag{9}$$

To obtain a fully discrete equation we apply the classical Galerkin weighted residual formulation to (9) and the resulting equations represent the ETG scheme for the particles convective transport problem in (3):

$$M\Delta N = B, \tag{10a}$$

$$M_{ij}^e = \iint_{\Omega^e}\left\{\phi_i^e\phi_j^e + \frac{\Delta t^2}{6}\left(v_x\frac{\partial\phi_i^e}{\partial x} + v_y\frac{\partial\phi_j^e}{\partial y}\right) \cdot\left(v_x\frac{\partial\phi_j^e}{\partial x} + v_y\frac{\partial\phi_i^e}{\partial y}\right)\right\}dx\,dy, \tag{10b}$$

$$B_i^e = -\Delta t\iint_{\Omega^e}\left(\phi_i^e + \frac{v_x\Delta t}{2}\frac{\partial\phi_i^e}{\partial x} + \frac{v_y\Delta t}{2}\frac{\partial\phi_i^e}{\partial y}\right)\left(v_x \cdot\frac{\partial N}{\partial x} + v_y\frac{\partial N}{\partial y}\right)dx\,dy, \tag{10c}$$

$$\begin{aligned} M &= \sum_{e=1}^{m}\left[M_{ij}^e\right], \\ B &= \sum_{e=1}^{m}\left[B_i^e\right], \\ &\qquad (i,j = 1,2,3), \end{aligned} \tag{10d}$$

where, denoting ϕ^e the element shape functions, m is the total of elements.

2.3. FCT Method. The essence of the FTC method is that a high-order flux and a low-order flux are merged into a weighted flux, which can decrease the numerical diffusion effectively. The details of the FCT method developed by Lohner et al. can be found in the literature [20]. The idea behind FCT is to assume that the density N^n and the velocity v are all known in the cell at time t_n. A high-order flux and a low-order flux can be obtained through variously different schemes in one time step Δt, and then we transform the solution of high- and low-order fluxes to obtain the number density at the next time $t_n + \Delta t$. Equations (10a), (10b), (10c), and (10d) as a high-order scheme are rewritten as follows:

$$M_c\Delta N^h = B^n. \tag{11}$$

Equation (11) is rewritten as follows:

$$\begin{aligned} M_L(\Delta N_r^n - \Delta N_{r-1}^n) &= B^n - M_c\Delta N_{r-1}^n \quad 1 \le r \le s, \\ M_L\Delta N^h &= B^n + (M_L - M_c)\Delta N^h, \end{aligned} \tag{12}$$

where ΔN_r is the vector of nodal increments and B^n is the vector of added element contributions to the nodes; ΔN_r^n denotes the rth iterate which in this paper is obtained for $r = s = 3$ and $\Delta N_0^n = 0$; M_c denotes the consistent mass matrix and M_L is the lumped mass matrix [17]. High-order flux adds diffusion coefficient, so the low-order flux is expressed as

$$M_L\Delta N^l = B^n + \text{Diff} = B^n + C_d(M_c - M_L)N^n, \tag{13}$$

where C_d is the diffusion coefficient and is assumed to be constant within the range 0-1. The high-order algorithm is, in essence, the Lax-Wendroff scheme, which is effectively explicit. This stability condition applied over an element e states that the time step Δt should satisfy

$$\Delta t < \frac{\lambda h_e}{|\omega_e|}, \tag{14}$$

where ω_e is the velocity in each element, h_e is the characteristic length of element e, and λ is taken to be 0.9 if one iteration is employed and 0.5 otherwise.

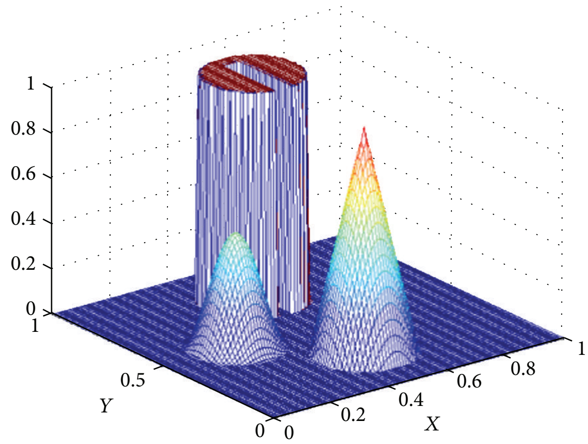

(a)

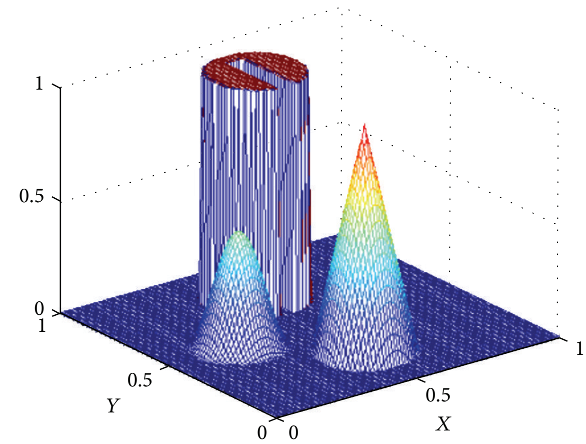

(b) ETG scheme

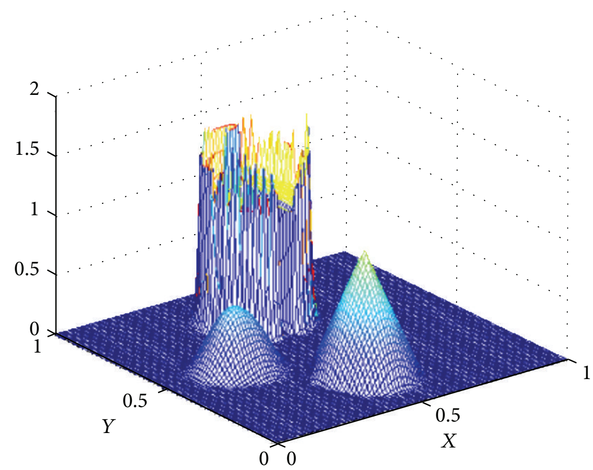

(c) LW-FDM

FIGURE 2: Numerical results for solid body rotation after one revolution (628 time steps) using the two schemes. (a) shows the accurate solution.

3. Numerical Tests

The performance of the ETG scheme is compared to the second-order Lax-Wendroff FDM (LW-FDM) [21], and it provides a good check on the performance of the present method before it is used for gas discharge problems in two dimensions. Rotation of solid bodies is frequently used to evaluate and compare numerical schemes for convection-dominated problems [22]. In order to examine the resolution of both smooth and discontinuous profiles, we consider the solid body rotation as proposed by Zalesak and LeVeque [21, 22]. Figure 2(b) shows the solution after a whole revolution obtained with the ETG scheme, whereas Figure 2(c) shows the corresponding results obtained with the LW-FDM scheme. Two different cross sections of the solution are depicted in Figure 3. It is clear that the two schemes of results are very similar and are found to be very close to the exact results. For this strongly time-dependent test problem, the ETG scheme performs much better on the steep gradients, which can be attributed to the use of the third-order Taylor series expansion. The LW-FDM can work well on very smooth data but has difficulties if results have steep gradients or discontinuous ones since it is very dispersive and tends to generate oscillations, also destroying the accuracy.

4. Simulation Results and Discussions

The simulation procedure consists of the following steps: (1) we give initial particle densities N^n and velocities at time t_n; (2) the electric field is calculated through the solution of Poisson's equation, and this is then used to update the transport parameters, such as ionization-collision coefficient, attachment coefficient, and diffusion coefficient; (3) the particle continuity equations are solved by ETG-FCT method. Moreover, we add ionization, attachment, migration, photoionization, and other processes. The particle densities and velocities are updated for time t_{n+1}. This procedure is repeated until the whole of the time domain is spanned.

The radius of the rod electrode is set at 0.25 mm. A rod-plate electrode configuration is used with a gap of 4 mm filled with 50~50% SF_6/N_2 mixed gas at atmospheric pressure (P = 0.1 Mpa) and a temperature of 300 K. The applied voltage to rod is −20 KV and the number density of SF_6/N_2 mixed gas is $2.467e^{25}$ m^{-3}. To keep the self-sustained discharge,

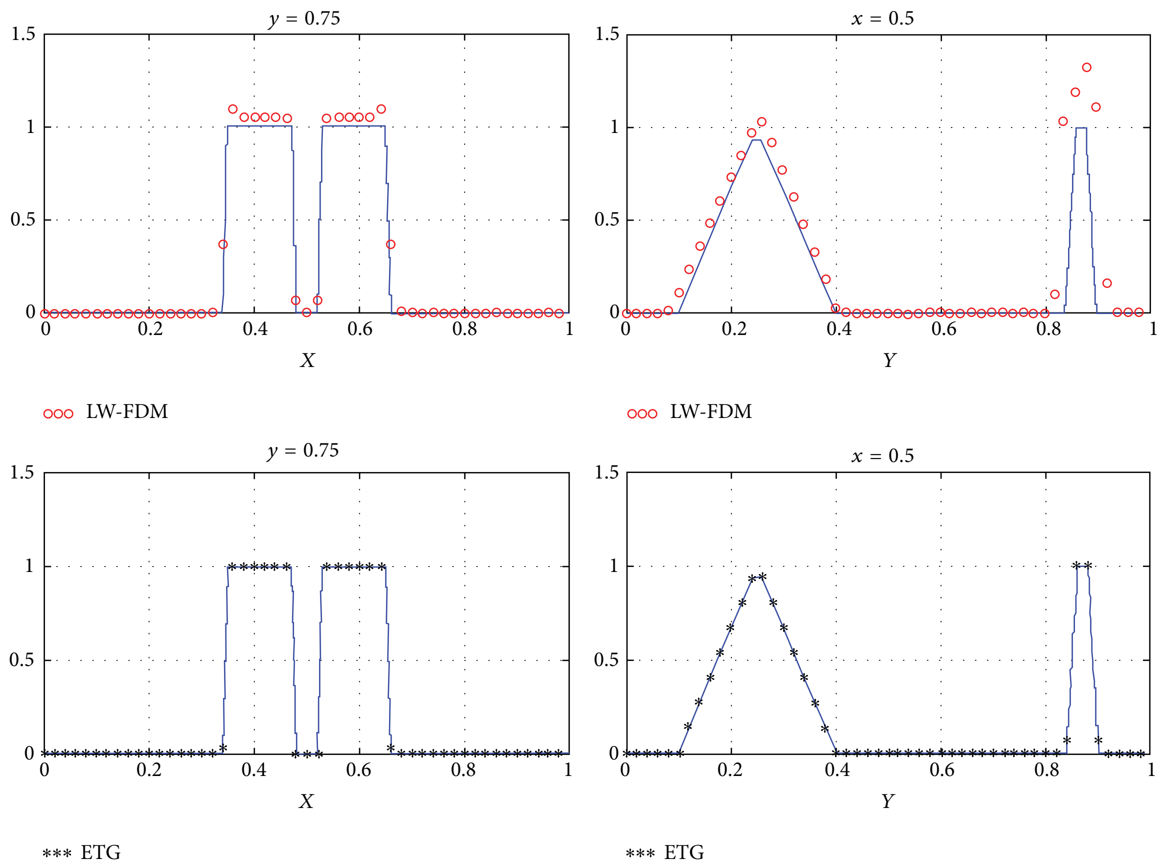

Figure 3: Two different cross sections of the solution are shown along with the perspective plot. The solid lines are the accurate solution.

the reduced electric field is $E > 343$ Td (1 Td = 10^{-21} V·m^2), and the effective ionization coefficient of SF_6/N_2 mixed gas is $(\alpha - \eta) > 0$; it is ensured that the plasma discharge growth reaches plate. Meanwhile, the calculation is initiated by approximately 10^{12} electrons released near the rod at $t = 0$ ns. Figures 4–7 show the spatial distributions of electrons densities, positive ions densities, negative ions densities, and photoelectrons densities, respectively.

In the rod-plate gap, the initial electrons in the plasma are accelerated by an electric field force. These electrons will collide with gas molecules knocking off new electrons, which in turn accelerate and create what is known as an electron avalanche. When the avalanche becomes “critical,” the space charge accumulation is high enough to distort the electric field. The expansion of the ionization in the avalanche leads to shielding charges and the formation of streamers. A streamer discharge occurs rapidly, so investigating it through experimental observations is difficult.

From Figure 4 it is found that, under the effect of electric field force, the electron cloud in the front of plasma head moves to the plate. The density of electron near the streamer head is about 10^{18} m^{-3} at $t = 1$ ns and remains to 10^{18}~10^{19} m^{-3} afterwards. Photoionization is one of the main factors promoting streamer propagation in gas mixtures [19]. From the figures it is found that the electron densities are lower than ion densities by an order of magnitude. That is because, on the one hand, there is recombination of positive ions and electrons. On the other hand, the SF_6 gas has strong attachment to electrons. Furthermore, the high field is further accelerating the ionization in space, the large second electrons generated by photoionization. Then electrons are mainly distributed near the plasma head.

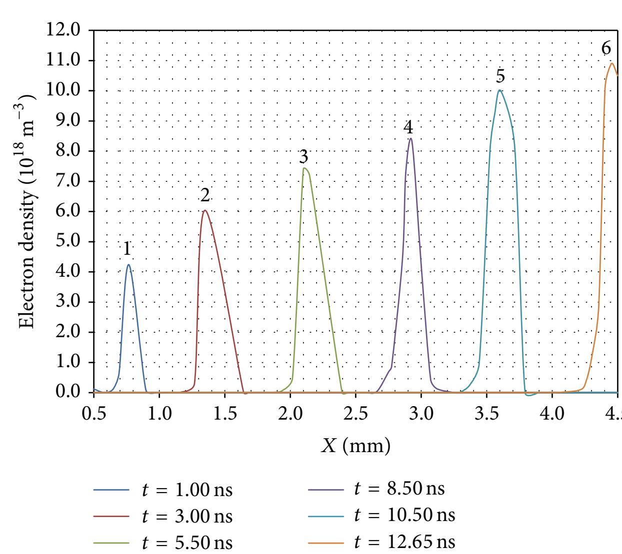

Figure 4: Electron density distributions on axis at different times.

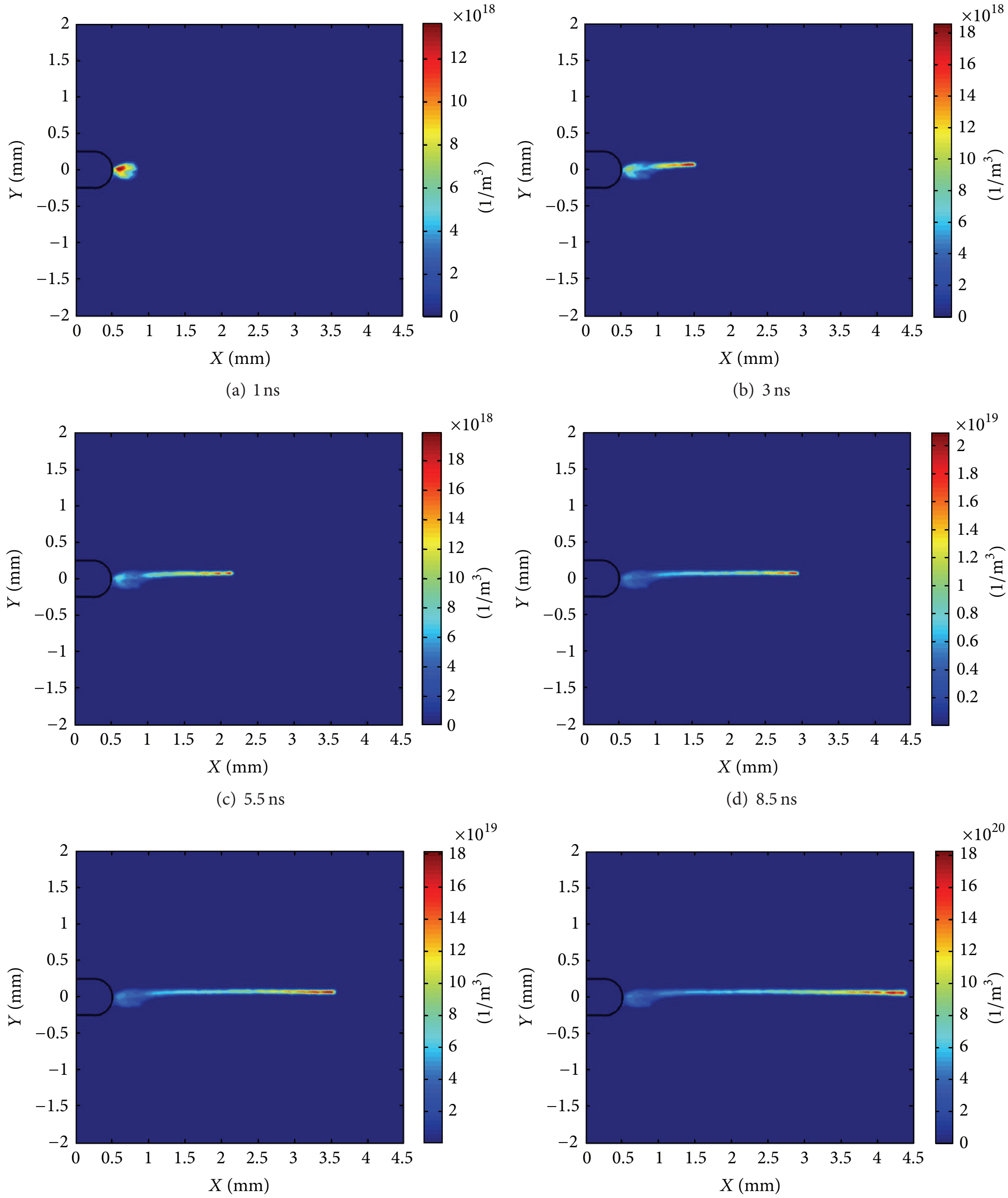

(a) 1 ns
(b) 3 ns
(c) 5.5 ns
(d) 8.5 ns
(e) 10.5 ns
(f) 12.65 ns

FIGURE 5: Negative ion density distributions (m^{-3}).

The ions velocity is much lower than those of electrons, and then they will separate in the streamer channel. In addition, the electron mobility is far greater than the ion mobility; there are a larger number of positive and negative ions when electrons pass through the space, and the ions number density keeps at about $10^{19}\ m^{-3}$ in the process of moving forward. Finally, the rod-plate gap is breakdown, the maximum negative ion densities of the plasma head are about $1.92e^{21}\ m^{-3}$, the maximum positive ion densities are about $1.96e^{21}\ m^{-3}$, and the maximum electron density is about $1.09e^{19}\ m^{-3}$. The order of magnitude of particle number density is shown to agree well with previously published reference [17]. The streamer bridges the whole gap in 12.65 ns, and its average velocity is around 32.2 cm/μs. In literature [23, 24], the average velocity of streamers is in the 10 cm/μs to 100 cm/μs range. Figures 5 and 6 show the streamer average

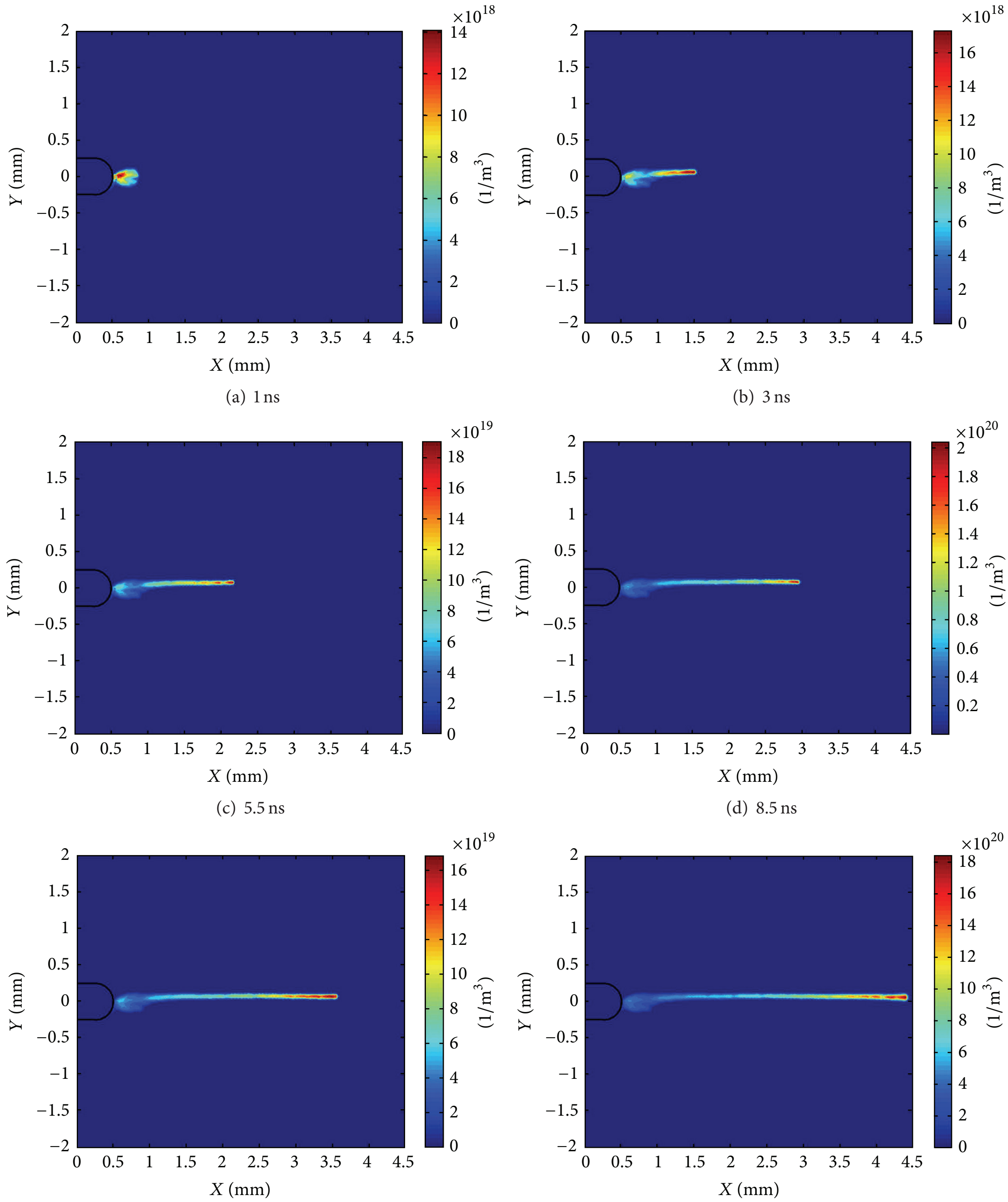

(a) 1 ns
(b) 3 ns
(c) 5.5 ns
(d) 8.5 ns
(e) 10.5 ns
(f) 12.65 ns

Figure 6: Positive ion density distributions (m^{-3}).

radius is about 0.18 mm. According to [24], the normal streamer mean radius is about 0.05~0.20 mm. It is found that the predicted streamer radius could vary depending on the starting conditions and this may account for some of the variability in streamer properties. Experimental conditions, such as gas number density, gap lengths, and electric field strengths, significantly affect the streamer propagation and formation.

Figure 8 shows the electric field distribution on axis at different times. From Figure 8 it is found that the electric field increases rapidly in different stages. The electric field at the plasma head is in the 310 Td to 650 Td range. This fast increase of electric field is due to the secondary electrons and photoelectrons generated from the collision ionization of neutrons by electrons. Furthermore, the charged densities are high enough to distort the field, so the maximum electric

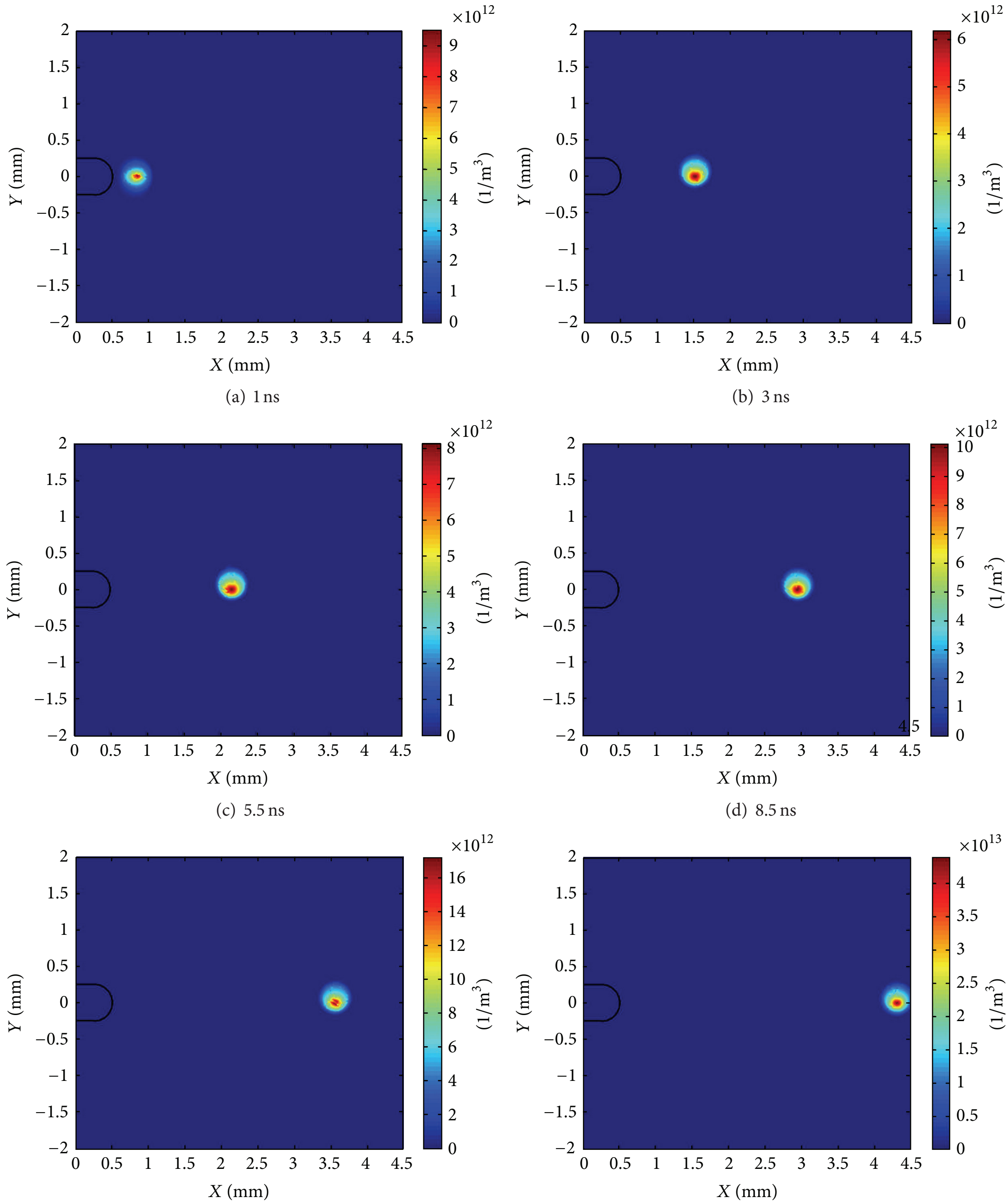

(a) 1 ns (b) 3 ns (c) 5.5 ns (d) 8.5 ns (e) 10.5 ns (f) 12.65 ns

Figure 7: Photoelectrons density distributions (m^{-3}).

field value is always near the plasma head in space. Figure 8 shows that the electric field distortion by space charge at t = 5.5 ns is more obvious than at t = 1 ns, but the maximum value of electric field is lower than that of t = 3 ns. It also shows that electric field is balanced by corona streamer. With the formation and growth of plasma, the space electric field of plasma head increases gradually, and the maximum value of space field is about 646.74 Td when the streamer reaches to plate.

5. Conclusions

The ETG scheme together with a FCT algorithm which is used for the solution of particle continuity transport

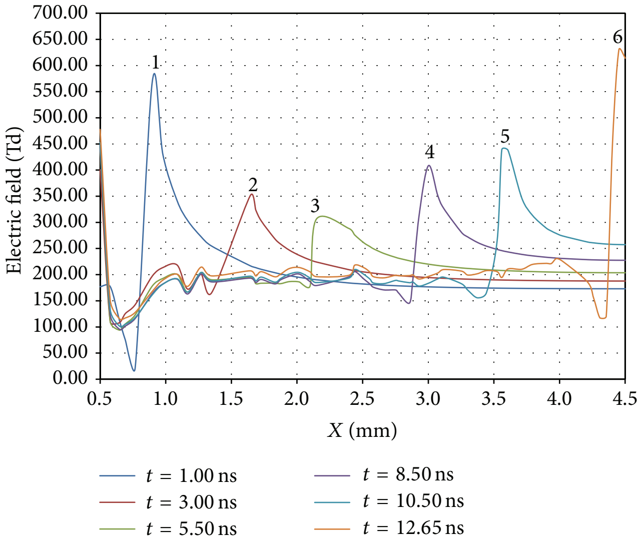

Figure 8: Electric field distributions on axis at different times.

equations in this paper can handle the convection term with steep gradients particularly well, improve calculation accuracy, and decrease the numerical diffusion effectively. The ETG-FCT scheme was used for the solution of a streamer problem, yielding the correct prediction of the plasma formation and growth. Meanwhile, the FEM has the advantage that nonuniformed triangular element girds can be used, which significantly reduces the number of nodes, resulting in considerable computational savings over the FDM.

In this study, the plasma discharge in SF_6/N_2 mixed gas is simulated by using 2D ETG-FCT method. Through this method, the electron densities, the ions densities, the photons densities, the electric field distribution, the velocity of plasma growth, and the radius of streamer can be obtained, respectively. From the results, it is found that the net charges play an important role in the process of the plasma formation and growth. The simulation results show that plasma weakens the electric field between the rod and the plasma and strengthens the electric field between the plate and it.

Conflict of Interests

The authors declare that there is no conflict of interests regarding the publication of this paper.

Acknowledgments

This study was supported in part by the Special Scientific Research Fund for Doctoral Subjects in Universities and Colleges (20120161110009). The authors wish to thank the Natural Science Foundation of Hunan Province, China (Grant no. 14JJ7029), and the National Natural Science Foundation of China (Grant no. 61102039).

References

[1] L. G. Christophorou and R. J. Van Brunt, “SF_6/N_2 Mixtures: basic and HV insulation properties,” *IEEE Transactions on Dielectrics and Electrical Insulation*, vol. 2, no. 5, pp. 952–1003, 1995.

[2] A. Moukengue Imano, R. Schurer, and K. Feser, “The influence of a conducting particle on a spacer on the insulation properties in SF_6/N_2 mixtures,” in *Proceedings of the 11th International Symposium on High Voltage Engineering*, vol. 3, pp. 232–235, London, UK, 1999.

[3] N. Bernard, S. Theoleyre, and G. Valentin, “How to use a greenhouse effect gas while being environmentally friendly: SF_6 case in medium voltage distribution,” in *Proceedings of the 16th International Conference and Exhibition on Electricity Distribution (CIRED ’01)*, IEE Conference Publication no. 481, Amsterdam, The Netherlands, June 2001.

[4] S. Singha and M. J. Thomas, “Very fast transient overvoltages in GIS with compressed SF_6-N_2 gas mixtures,” *IEEE Transactions on Dielectrics and Electrical Insulation*, vol. 8, no. 4, pp. 658–664, 2001.

[5] D. H. Rhie and H. J. Seo, “Spark discharge characteristics of various SF_6-based binary gases in non-uniform fields,” in *Proceedings of the International Conference on Energy & Environmental Systems*, pp. 328–332, Chalkida, Greece, 2006.

[6] C. M. Franck, D. A. Dahl, M. Rabie, P. Haefliger, and M. Koch, “An efficient procedure to identify and quantify new molecules for insulating gas mixtures,” *Contributions to Plasma Physics*, vol. 54, no. 1, pp. 3–13, 2014.

[7] J. P. Boris and D. L. Book, “Flux-corrected transport. I. SHASTA, a fluid transport algorithm that works,” *Journal of Computational Physics*, vol. 11, no. 1, pp. 38–69, 1973.

[8] A. J. Davies, C. S. Davies, and C. J. Evans, “Computer simulation of rapidly developing gaseous discharges,” *IEE Proceedings of Science, Measurement and Technology*, vol. 118, pp. 816–823, 1971.

[9] C. Montijn, W. Hundsdorfer, and U. Ebert, “An adaptive grid refinement strategy for the simulation of negative streamers,” *Journal of Computational Physics*, vol. 219, no. 2, pp. 801–835, 2006.

[10] V. John and J. Novo, “On (essentially) non-oscillatory discretizations of evolutionary convection–diffusion equations,” *Journal of Computational Physics*, vol. 231, no. 4, pp. 1570–1586, 2012.

[11] C. Zhuang, R. Zeng, B. Zhang, S. Chen, and J. He, “Accelerating the convergence of algebraic multigrid for quadratic finite element method by using grid information and p-multigrid,” *IEEE Transactions on Magnetics*, vol. 47, no. 5, pp. 1198–1201, 2011.

[12] Y. I. Bychkov and A. G. Yastremskii, “Kinetic processes in the electric discharge in SF6,” *Laser Physics*, vol. 16, no. 1, pp. 146–154, 2006.

[13] D. V. Beloplotov, M. I. Lomaev, D. A. Sorokin, and V. F. Tarasenko, “Diffuse and spark discharges at high overvoltages in high pressure air, nitrogen, and SF_6,” *Development and Applications of Oceanic Engineering*, vol. 3, pp. 39–45, 2014.

[14] R. Morrow, “Theory of positive corona in SF_6 due to a voltage impulse,” *IEEE Transactions on Plasma Science*, vol. 19, no. 2, pp. 86–94, 1991.

[15] W. Pfeiffer, L. Tong, and D. Schoen, “Computer simulation of plasma discharge processes in SF_6 and SF_6/N_2 mixtures,” in *Proceedings of the 14th International Conference on Gas Discharges and Their Applications*, pp. 227–230, Liverpool, UK, 2002.

[16] A. Hallac, G. E. Georghiou, and A. C. Metaxas, “Streamer branching in transient nonuniform short gap discharges using

numerical modeling," *IEEE Transactions on Plasma Science*, vol. 33, no. 2, pp. 266–267, 2005.

[17] Y. Zhang, R. Zeng, X.-L. Li et al., "Numerical simulation on streamer discharge of short air gap of atmospheric air," *Proceedings of the Chinese Society of Electrical Engineering*, vol. 28, no. 28, pp. 6–12, 2008 (Chinese).

[18] S. Kacem, O. Eichwald, O. Ducasse, N. Renon, M. Yousfi, and K. Charrada, "Full multi grid method for electric field computation in point-to-plane streamer discharge in air at atmospheric pressure," *Journal of Computational Physics*, vol. 231, no. 2, pp. 251–261, 2012.

[19] A. Bourdon, V. P. Pasko, N. Y. Liu, S. Célestin, P. Ségur, and E. Marode, "Efficient models for photoionization produced by non-thermal gas discharges in air based on radiative transfer and the Helmholtz equations," *Plasma Sources Science and Technology*, vol. 16, no. 3, pp. 656–678, 2007 (Chinese).

[20] R. Lohner, K. Morgan, J. Peraire, and M. Vahdati, "Finite element flux-corrected transport (FEM-FCT) for the Euler and Navier–Stokes equation," *International Journal for Numerical Methods in Fluids*, vol. 17, pp. 1093–1109, 1987.

[21] S. T. Zalesak, "Fully multidimensional flux-corrected transport algorithms for fluids," *Journal of Computational Physics*, vol. 31, no. 3, pp. 335–362, 1979.

[22] R. J. LeVeque, "High-resolution conservative algorithms for advection in incompressible flow," *SIAM Journal on Numerical Analysis*, vol. 33, no. 2, pp. 627–665, 1996.

[23] T. Mizobuchi, H. Toyota, S. Matsuoka, A. Kumada, and K. Hidaka, "Nanosecond electrical discharge development in SF_6-N_2 gas mixtures," *IEEJ Transactions on Fundamentals and Materials*, vol. 125, pp. 629–635, 2005.

[24] R. Morrow, "Properties of streamers and streamer channels in SF_6," *Physical Review A*, vol. 35, no. 4, pp. 1778–1785, 1987.